



Quantifying Intracranial Plaque Permeability with Dynamic Contrast-Enhanced MRI: A Pilot Study

P. Vakil, A.H. Elmokadem, F.H. Syed, C.G. Cantrell, F.H. Dehkordi, T.J. Carroll and S.A. Ansari

This information is current as of June 25, 2025.

AJNR Am J Neuroradiol 2017, 38 (2) 243-249

doi: <https://doi.org/10.3174/ajnr.A4998>

<http://www.ajnr.org/content/38/2/243>

Quantifying Intracranial Plaque Permeability with Dynamic Contrast-Enhanced MRI: A Pilot Study

 P. Vakil,  A.H. Elmokadem,  F.H. Syed,  C.G. Cantrell,  F.H. Dehkordi,  T.J. Carroll, and  S.A. Ansari



ABSTRACT

BACKGROUND AND PURPOSE: Intracranial atherosclerotic disease plaque hyperintensity and/or gadolinium contrast enhancement have been studied as imaging biomarkers of acutely symptomatic ischemic presentations using single static MR imaging measurements. However, the value in modeling the dynamics of intracranial plaque permeability has yet to be evaluated. The purpose of this study was to use dynamic contrast-enhanced MR imaging to quantify the contrast permeability of intracranial atherosclerotic disease plaques in symptomatic patients and to compare these parameters against existing markers of plaque volatility using black-blood MR imaging pulse sequences.

MATERIALS AND METHODS: We performed a prospective study of contrast uptake dynamics in the major intracranial vessels proximal and immediately distal to the circle of Willis using dynamic contrast-enhanced MR imaging, specifically in patients with symptomatic intracranial atherosclerotic disease. Using the Modified Tofts model, we extracted the volume transfer constant (K^{trans}) and fractional plasma volume (V_p) parameters from plaque-enhancement curves. Using regression analyses, we compared these parameters against time from symptom onset as well as intraplaque hyperintensity and postcontrast enhancement derived from T1 SPACE, a black-blood MR vessel wall imaging sequence.

RESULTS: We completed analysis in 10 patients presenting with symptomatic intracranial atherosclerotic disease. K^{trans} and V_p measurements were higher in plaques versus healthy white matter and similar or less than values in the choroid plexus. Only K^{trans} correlated significantly with time from symptom onset ($P = .02$). Dynamic contrast-enhanced MR imaging parameters were not found to correlate significantly with intraplaque enhancement or intraplaque hyperintensity ($P = .4$ and $P = .17$, respectively).

CONCLUSIONS: Elevated K^{trans} and V_p values found in intracranial atherosclerotic disease plaques versus healthy white matter suggest that dynamic contrast-enhanced MR imaging is a feasible technique for studying vessel wall and plaque characteristics in the proximal intracranial vasculature. Significant correlations between K^{trans} and symptom onset, which were not observed on T1 SPACE–derived metrics, suggest that K^{trans} may be an independent imaging biomarker of acute and symptom-associated pathologic changes in intracranial atherosclerotic disease plaques.

ABBREVIATIONS: BBMRI = black-blood MRI; DCE = dynamic contrast-enhanced; GRE = gradient recalled-echo; ICAD = intracranial atherosclerotic disease; IPE = intraplaque enhancement; IPH = intraplaque hyperintensity; K^{trans} = volume transfer constant; NAWM = normal-appearing white matter; SPACE = sampling perfection with application-optimized contrasts by using different flip angle evolution; SI = signal intensity; V_L = extracellular extravascular space; V_p = fractional plasma volume

Stroke is the third leading cause of death in the United States, with an incidence of approximately 800,000 per year. Intra-

cranial atherosclerotic disease (ICAD) is responsible for approximately 7%–10% of these patients; however, the risk of recurrent stroke in this population approaches nearly 12%–25% over 1–2 years, despite aggressive medical management including anti-


Received April 4, 2016; accepted after revision August 22.

From the College of Medicine (P.V.), University of Illinois, Chicago, Illinois; Departments of Radiology (P.V., A.H.E., F.S., C.G.C., T.J.C., S.A.A.), Biomedical Engineering (P.V., C.G.C., T.J.C.), and Neurology and Neurological Surgery (S.A.A.), Northwestern University, Chicago, Illinois; and Department of Economics and Decision Sciences (F.H.D.), Western Illinois University, Macomb, Illinois.

This work was supported by the following grants: American Heart Association 13GRNT17340018 and 14GRNT20380798 (Principal Investigators: S.A. Ansari and T.J. Carroll); PRE20380810 (Principal Investigator: C.G. Cantrell); National Institutes of Health 1R21HL130969 (Principal Investigator: S.A. Ansari); 1R01NS089926 and 1R21EB017928 (Principal Investigator: T.J. Carroll).

Paper previously presented in part at: Annual Meeting of the European Congress of Radiology, March 2–6, 2016; Vienna, Austria and Annual Meeting of the American Society of Neuroradiology, May 23–26, 2016; Washington, DC. The abstract was published in *Insights Imaging* 2016;7:162. doi:10.1007/s13244-016-0475-8

Please address correspondence to Sameer A. Ansari, MD, PhD, Departments of Radiology, Neurology, and Neurological Surgery, Northwestern University, Feinberg School of Medicine, 676 N St. Clair St, Suite 800, Chicago, IL 60611-2927; e-mail: s-ansari@northwestern.edu

 Indicates open access to non-subscribers at www.ajnr.org

<http://dx.doi.org/10.3174/ajnr.A4998>

platelet or antithrombotic medications.^{1,2} ICAD risk assessment for ischemic complications based on a simple degree of luminal narrowing (percentage stenosis) is imprecise, with complex pathology at the level of the plaque and/or downstream vascular distribution. Several groups have proposed improving patient risk stratification and plaque characterization by using black-blood MR imaging (BBMRI) with high (submillimeter) spatial and contrast resolution to directly analyze the intracranial vessel wall and atherosclerotic plaque.^{3–6} Swartz et al³ initially reported contrast enhancement of symptomatic ICAD plaques with 3T high-resolution BBMRI; later in a small cohort, they demonstrated qualitatively decreasing enhancement of symptomatic plaques from acute/subacute-to-chronic phases, suggesting plaque inflammation and transient destabilization as an etiology for thromboembolic complications.⁴

While ICAD plaque enhancement has been shown to be highly associated with recent cerebrovascular ischemic events, its specificity remains uncertain. Using postcontrast BBMRI, Qiao et al⁷ reported observing intracranial plaque enhancement in both culprit (the most stenotic lesion upstream from an ischemic event) and nonculprit lesions in patients with cerebrovascular events. Skarpathiotakis et al⁴ reported “strong” ICAD plaque enhancement on postcontrast BBMRI, even 4 months after stroke presentation, and “mild” enhancement as much as 1 year later.

The concept of introducing additional quantitative MR imaging parameters by using dynamic contrast-enhanced (DCE) MR imaging to measure adventitial contrast uptake rates, represented by the volume transfer constant (K^{trans}), was first introduced by Kerwin et al⁸ in patients with carotid atherosclerotic disease requiring surgical endarterectomy. These parameters were found to correlate with macrophage infiltration (inflammation) and neovasculature on subsequent histopathologic analysis.^{8–10} In a separate cohort, Dong et al¹¹ demonstrated that intensive medical management with lipid therapy coincided with a significant decrease in the measured K^{trans} of carotid artery atherosclerosis. In fact, K^{trans} measurements decreased in intervals and responded to medical management with anticholesterolemic (statin) medications during 1 year of therapy, suggesting correlative reduction in neovascularization and/or inflammation, plaque stabilization, and even regression.¹¹

These plaque perfusion parameters may provide information that is also correlated to intracranial plaque inflammation, indicative of both ischemic stroke risk and sensitivity to pharmacologic therapies. Chen et al¹² demonstrated neovascularization in MCA plaques in a postmortem study, suggesting applicability of DCE kinetic modeling to the intracranial vasculature; however, to date, no study has examined the dynamic characteristics of intracranial vessel walls or ICAD plaques using DCE-MR imaging. In this pilot study, we investigated the feasibility of modeling plaque perfusion parameters, fractional plasma volume (V_p), and K^{trans} , using DCE-MR imaging in patients with symptomatic ICAD. We hypothesized that kinetic modeling of the intracranial vessel wall and plaque provide quantitative biomarkers sensitive to time from symptom onset of ICAD, independent of relative T1 signal hyperintensity and post-gadolinium enhancement values as observed on BBMRI.

Table 1: Patient demographics^a

Characteristics	Value
Age (mean) (yr)	58.9 ± 10
Sex	
Male	6
Female	4
Active smoker	3
Alcohol	2
Antiplatelets	9
Statins	8
Hypertension	5
Diabetes mellitus	6
Dyslipidemia	5
Atrial fibrillation	0
Coronary artery disease	1
Neurologic symptoms	10
Imaging data	
DWI+	9
Watershed	4
Perforator	4
Both	1
Vessel	
MCA	8
PCA	1
ICA	1

Note:—PCA indicates posterior cerebral artery.

^a Data are numbers unless otherwise indicated.

MATERIALS AND METHODS

Patient Recruitment

Institutional review board approval was obtained for a prospective, Health Insurance Portability and Accountability Act–compliant study of symptomatic patients presenting with ischemic stroke or transient ischemic attack secondary to ICAD with >50% stenosis and plaques involving the internal carotid artery, A1–A2 anterior cerebral, M1–M2 middle cerebral, and P1–P2 posterior cerebral arteries, or basilar artery (Table 1). When attributable to the downstream vascular distribution of a single ICAD plaque, “ischemic stroke” was defined as hyperintensity findings on DWI and “TIA” was defined as neurologic deficits that resolved in <24 hours. Patients were identified and recruited for this study at Northwestern University from March 2013 to May 2015, after receiving a standard clinical head and neck MRI/MRA evaluation, including 3D TOF and DWI sequences. Patients provided consent based on a willingness to participate in a longitudinal study and the ability to undergo a research MR imaging examination within 30 days of the ischemic event.

Recruited patients underwent high-resolution, vessel wall imaging with 3T BBMRI of the intracranial vasculature. In addition, the ICAD stenosis was evaluated with DCE-MR imaging for the purpose of kinetic modeling of permeability (or contrast uptake) into the plaque. Major patient exclusion criteria included complete vessel occlusions, gross patient motion artifacts, susceptibility artifacts from implants, >50% stenosis of the cervical vasculature or tandem intracranial stenoses (via MRA/CTA or carotid Doppler sonography), cardioembolic risk profile including atrial fibrillation, and standard contraindications to MR imaging (pacemaker, claustrophobia, pregnancy, contrast allergy, or renal insufficiency). We further studied patient demographics, atherosclerotic risk factors, relevant medical management, and clinical presentations using Northwestern University’s electronic medical records.

Imaging Protocol

All patients enrolled in our study were scanned on 3T (Magnetom Trio or Skyra; Siemens, Erlangen, Germany) MR imaging scanners. A 3D TOF MRA sequence was repeated to localize the ICAD plaque in the vessel of interest. The DCE-MR imaging volume was placed to cover the entire segment of the diseased intracranial vessel (Fig 1) with the axis of the vessel aligning with the through-plane direction and in-plane images containing perpendicular vessel cross-sections. Plaque permeability was measured with a standard DCE-MR imaging protocol using a multiphase 3D gradient recalled-echo (GRE)-based pulse sequence. Dynamic volumetric T1-weighted images were acquired approximately every 35 seconds following contrast injection for approximately 10 minutes with the following parameters: flip angle = 10°, TR/TE = 8.7/1.3 ms, matrix = 384 × 384, FOV = 190–220 mm, and 12 partitions placed to cover the plaque, resulting in voxel dimensions of 0.5 × 0.5 × 2.0 mm. A single dose (0.1 mmol/kg) of T1-shortening gadolinium contrast (gadopentetate dimeglumine, Magnevist; Bayer HealthCare Pharmaceuticals, Wayne, New Jersey) was injected at a rate of 4 mL/s during the DCE acquisition. Precontrast T1 values (T_{10}) of the tissue were determined using a multi-flip angle routine ($\alpha = 5^\circ, 15^\circ, 25^\circ, 45^\circ$) to fit the spoiled gradient-echo signal equation:^{13,14}

$$1) \quad S(\alpha) = A \sin \alpha \frac{1 - \exp(-TR/T_{10})}{1 - \cos \alpha \exp(-TR/T_{10})}.$$

3D isotropic, high-resolution BBMRI was performed with T1-weighted TSE sequences, acquired before and immediately after the DCE acquisition (ie, within 20 minutes of the gadolinium injection). A 3D variable flip angle TSE (T1 sampling perfection with application-optimized contrasts by using different flip angle evolution [SPACE]; Siemens) pulse sequence^{5,15} was performed before and after contrast injection with the following parameters: FOV = 165 mm, TR/TE = 800/22 ms, integrated parallel acquisition technique factor = 2, 104 partitions, bandwidth = 372 Hz/pixel, turbo factor = 30, scan time ~ 8 minutes, voxel volume = 0.5 × 0.5 × 0.6 mm.

Permeability Modeling

The permeability-limited Modified Tofts Model¹⁶ quantifies the kinetics of a tracer leaking through a semipermeable membrane with the following relationship:

$$2) \quad C(t) = K^{\text{trans}} \int_0^t e^{-K_{\text{ep}}(t-\tau)} C_p(\tau) d\tau + V_p C_p(t),$$

with K^{trans} dictating the tracer transfer rate from the intravascular into the extracellular extravascular space (V_L) with units of min^{-1} ; $K_{\text{ep}} = K^{\text{trans}}/V_L$ in units of min^{-1} describing the ratio of the transfer rate (K^{trans}) to the fractional volume of tracer in the V_L ; $C_p(t)$, the intravascular tracer concentration; and V_p , the fractional plasma volume for each voxel. $C(t)$ is measured adjacent to the patent lumen of the stenotic vessel wall. A Levenberg-Marquardt algorithm was implemented in-house by using a commercially available software prototyping package (Matlab, Version 2014; MathWorks, Natick, Massachusetts) to find the K^{trans} , V_L , and V_p in Equation 2 that best fit the measured signal $C(t)$. Acquisition of the enhancement curve peak is required for an accu-

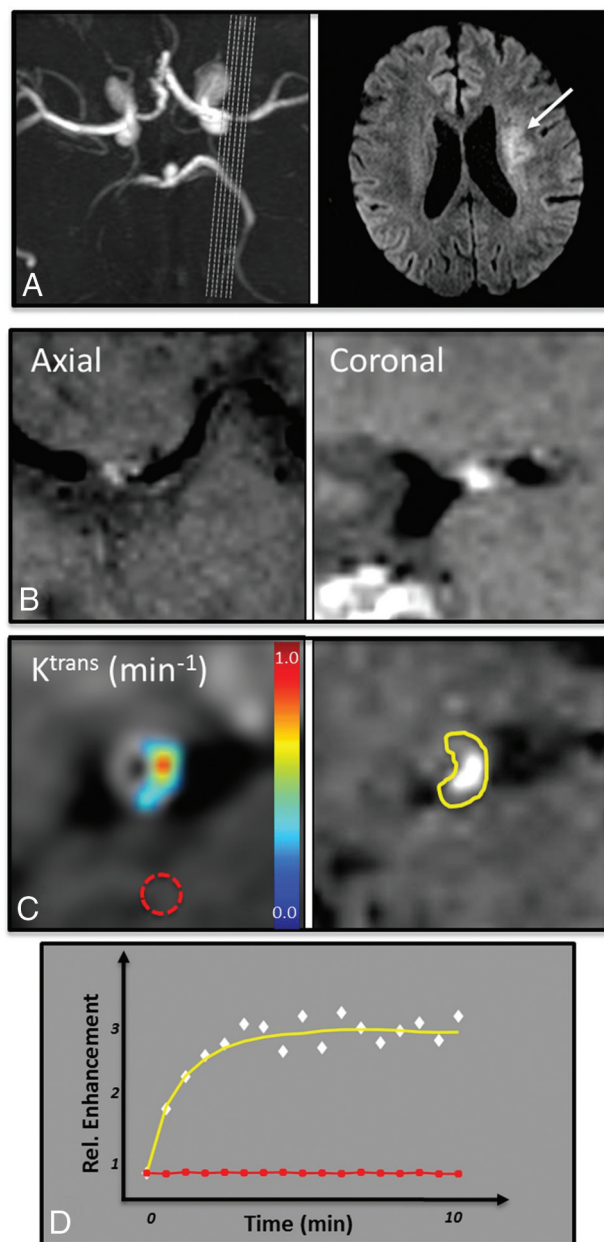


FIG 1. Vessel wall imaging data in a 63-year-old man with symptomatic severe left MCA stenosis resulting in perforator thromboembolic infarcts as seen on 3D TOF MRA MIP and DWI (A). 3D BBMRI with postcontrast T1 SPACE imaging demonstrates plaque enhancement in an axial and coronal cross-sections of the MCA (B). A manual ROI isolates the enhancing plaque on the postcontrast T1 SPACE image (C, right, yellow ROI on the plaque inset). Kinetic modeling of contrast uptake into the plaque was performed by using DCE-MR imaging in the coregistered plaque ROI, and K^{trans} values were calculated in each voxel (C, left). Normal control values were calculated in a region of normal white matter (red dotted ROI in C). The mean enhancement signal (white diamonds) and fitted Tofts curve (yellow) are shown from the plaque ROI (D). Note the difference in enhancement relative to healthy brain tissue (D, red ROI and red curve/squares).

rate measurement of V_L and may require imaging times greater than 10 minutes. While V_L may be related to plaque enhancement, it does not affect the wash-in phase of the enhancement curve¹⁷; thus, we restricted our analysis to K^{trans} and V_p values as in prior kinetic modeling analyses.^{7,9}

Data Analysis and Imaging Evaluation

Both DCE and T1 SPACE images were evaluated as a postprocessing step by separate, independent operators who were blinded to both clinical history and the results of complementary image analysis.

T1 SPACE images were analyzed on a Leonardo workstation (Siemens) by a neuroradiologist with >10 years' experience (A.H.E). Measurements included relative postgadolinium plaque enhancement between pre- and postcontrast imaging, referred to as intraplaque enhancement (IPE), as well as the presence of pre-contrast signal intensity (SI), referred to as intraplaque hyperintensity (IPH). ROIs were drawn in one section at the site of maximal vessel stenosis, and the mean SI was recorded. ROIs were matched in size and location in the precontrast T1 SPACE dataset. IPE was calculated as $SI_{\text{post}} - SI_{\text{pre}} / SI_{\text{pre}}$. Both SI_{post} and SI_{pre} were first normalized to the SI of normal-appearing white matter (NAWM). IPH was measured as the ratio of precontrast plaque SI to extraocular muscle SI.

DCE images were motion-corrected by using the Statistical Parametric Mapping (SPM8 (<http://www.fil.ion.ucl.ac.uk/spm/software/spm12>)) software package in Matlab (R2014a). The ROI for contrast kinetic analysis was matched as closely as possible to the ROI used for IPE analysis by first coregistering the T1 SPACE postcontrast ROI volumes to DCE-MR imaging volumes and then applying pixel-by-pixel DCE modeling in the section containing maximal plaque enhancement on the coregistered T1 SPACE image. ROIs were drawn in Matlab by a trained operator with >10 years' experience (P.V.). We evaluated the permeability of the choroid plexus and NAWM¹⁸⁻²⁰ in the same patients to

provide an internal reference for our plaque contrast kinetic parameters.

Statistical Analysis

We compared quantitative DCE-MR imaging parameters in plaques against the aforementioned independent controls (white matter and choroid plexus) and neuroanatomic structures with differential permeability characteristics.^{18,19,21-23} Mean values were compared by using a Student *t* test with statistical significance defined at the 5% level ($P < .05$).

A linear regression analysis was performed to compare DCE parameters (K^{trans} and V_p) as well as IPH and IPE ratios with the time from symptom onset (in days). Time from symptom onset was calculated as the number of days until DCE and T1 SPACE MR imaging studies were performed at our research institution. This analysis was conducted to evaluate the difference in associativity with time between the 2 imaging markers.

Finally, DCE parameters were compared with IPH and IPE ratios in all plaques by using linear regression to evaluate their interdependent relationships. All statistical analyses were conducted by using built-in statistical software in Matlab. Confidence intervals were set at 95%, and statistical significance was defined at the 5% level ($P < .05$).

RESULTS

We evaluated 10 consecutive symptomatic patients (6 men, 4 women; mean age, 58.9 years; range, 39–70 years) with ICAD plaques by using DCE and T1 SPACE MR imaging. Patient demographics, comorbid atherosclerotic risk factors, relevant medical management, and clinical presentations are summarized in Table 1. In addition, 14 other patients were recruited for scanning but were excluded from this study: 2 with documented complete vessel occlusions in the plaque ROI, 3 with nondiagnostic imaging due to patient motion artifacts, and 9 with confounding tandem or distal plaques in the vessel of interest.

We found a broad-range of K^{trans} and V_p values in ICAD plaques (Table 2). In our cohort, mean plaque K^{trans} was 0.31 ± 0.14 minutes⁻¹, ranging from 0.11 to 0.53 minutes⁻¹. A Student *t* test found that plaque K^{trans} was significantly smaller than the uptake rates in the choroid plexus (mean, 0.47 minutes⁻¹; $P = .0037$) and larger

than values measured in NAWM (mean, 0.0031 minutes⁻¹; $P = 2.3E-06$). Similarly, average plaque V_p was $18.3\% \pm 10.2\%$; range, 5%–40%, and it was significantly smaller than the mean values found in the choroid plexus (mean, 44%; $P = 6.8E-06$) and larger than mean values measured in NAWM (mean, 1.9%; $P = 9.4E-05$) (Fig 2).

Linear regression modeling of DCE plaque permeability parameters and T1 SPACE IPH and IPE ratios demonstrated that K^{trans} was most associated with time from symptom onset in days ($r^2 = 0.46$, $P = .03$), but vascular fraction V_p ($r^2 = 0.12$, $P = .3$), IPH ($r^2 = 0.07$, $P = .47$), and IPE ($r^2 = 0.005$, $P = .95$) ratios did not correlate significantly (Fig 3).

Table 2: Quantitative imaging findings

Subject	K^{trans} (min ⁻¹)	V_p (%)	IPE (%)	IPH (%)
1	0.53	20	230	84
2	0.12	24	131	58
3	0.11	5	181	8
4	0.24	20	159	38
5	0.20	9	215	46
6	0.39	11	123	80
7	0.28	16	99	89
8	0.33	40	294	25
9	0.45	12	226	32
10	0.41	26	175	82

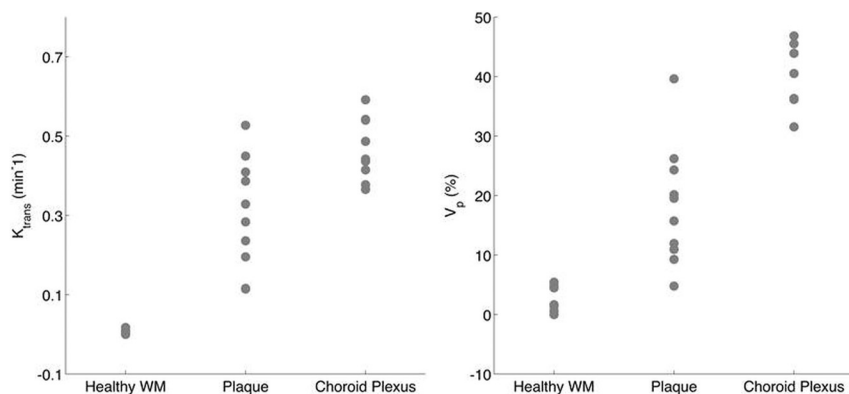


FIG 2. K^{trans} and V_p values are shown for ICAD plaques and compared against the paired choroid plexus and NAWM measured in the same subjects. Both mean plaque K^{trans} and V_p values were diverse and significantly different from choroid plexus and healthy white matter values (see text for relevant *P* values).

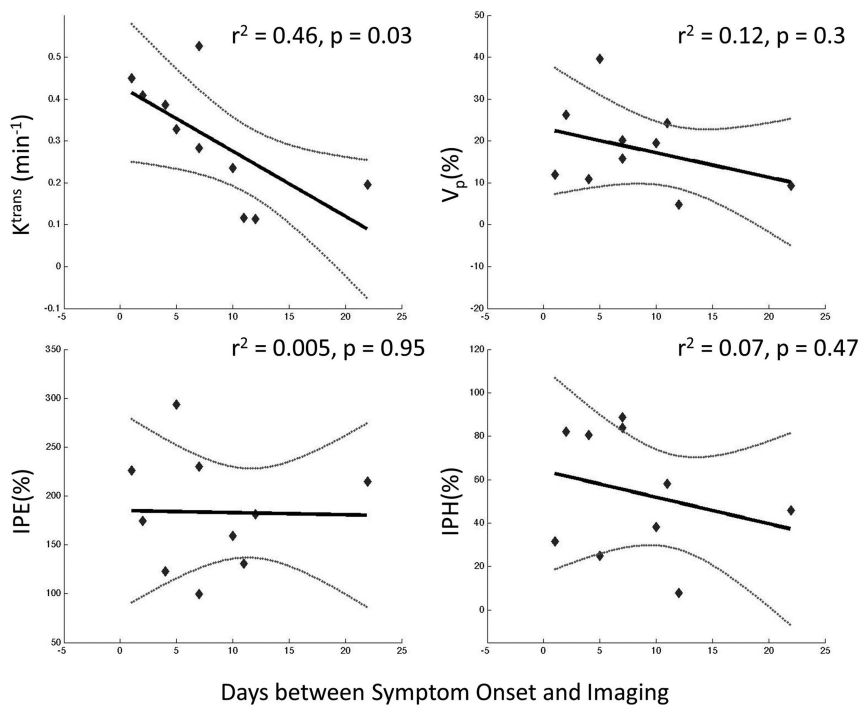


FIG 3. Linear regression analysis demonstrates that K^{trans} and V_p measured on DCE-MR imaging are more correlated (r^2 and P values) to time from symptom onset than intraplaque contrast enhancement and precontrast hyperintensity measured on T1 SPACE imaging. K^{trans} is the most associated and significant in its correlation ($r^2 = 0.46$ and $P = .03$).

DCE and T1 SPACE parameters did not correlate significantly with one another: K^{trans} versus IPE ($r^2 = 0.101$, $P = .4$); K^{trans} versus IPH ($r^2 = 0.221$, $P = .17$); V_p versus IPE ($r^2 = 0.16$, $P = .3$); and V_p versus IPH ($r^2 = 0.007$, $P = .818$). This finding is illustrated in Fig 4, which shows representative imaging in 2 patients, with 226% versus 122% IPE ratios. In contrast, despite this nearly 2-fold difference in IPE between the cases, K^{trans} levels remained consistently high at 0.39 minutes⁻¹ and 0.45 minutes⁻¹, respectively.

DISCUSSION

In this pilot study, we demonstrated the feasibility of kinetic modeling of contrast uptake in ICAD plaques. Enhancement curve shapes and K^{trans}/V_p values were consistent with literature values reported in DCE studies on extracranial carotid plaques^{8,10} and intermediate to values found in the healthy white matter (NAWM) and the choroid plexus. Furthermore, we found that DCE permeability parameters showed little correlation to IPE and IPH values derived from T1 SPACE imaging and demonstrated greater correlation with time from symptom onset. Our findings suggest that contrast kinetics modeled by DCE-MR imaging allows intracranial plaque characterization that differs from pre- and postcontrast plaque signal or enhancement seen with static vessel wall imaging protocols using BBMRI.

The strong relationship between K^{trans} and time from symptom onset may be evidence of the correlation of contrast kinetics to acute pathophysiologic changes occurring after the destabilization of intracranial plaques and thromboembolic conversion. Our data did not demonstrate similar temporal correlation with respect to IPE or IPH, consistent with recent intracranial vessel wall imaging studies that showed persistent and strong en-

hancement in ICAD plaques as much as 6 months after symptom onset. Additional studies that follow symptomatic and asymptomatic plaques longitudinally will be essential to establishing whether contrast uptake rates into the vessel wall provide a more specific and acute measure of plaque stability than static measures of pre- and postcontrast signal or enhancement.

Studies by Kerwin et al¹⁸ have shown that DCE-MR imaging can provide a surrogate measure of plaque inflammation by visualizing the rate of intercompartmental exchange of contrast from the extracranial carotid vaso vasorum into the adjacent extracellular extravascular spaces within an atherosclerotic lesion. These rates, modeled as K^{trans} , correlated with macrophage infiltration and percentage neovascularization on histopathologic analysis. Increasing evidence indicates the role of neovascularization, ruptured thrombogenic lipid core, intraplaque hemorrhage, and recruitment of inflammatory cells (macrophages) in the

progression and rupture of carotid atherosclerotic plaques, analogous to the coronary literature.²⁴⁻²⁶ An analogous relationship of high intracranial plaque K^{trans} values to intracranial plaque destabilization and thromboembolic complications can be postulated. Although intracranial vessel wall pathology may have similar responses to progressing atherosclerotic disease, the non-pathologic absence of the vaso vasorum and an external elastic lamina in the intracranial vasculature may result in different pathophysiologic responses and hence contrast kinetics in symptomatic ICAD.

Despite inflammation leading to acute instability of an ICAD plaque, existing data on plaque K^{trans} values with associated neovascularization and macrophage infiltration are derived from carotid endarterectomy studies with histopathologic confirmation. Because these studies are not feasible in ICAD except in postmortem specimens, an alternative approach may be to correlate plaque K^{trans} values against GRE T2⁺- or T2 SPACE-weighted imaging of intracranial plaque following ferumoxytol infusion. Hasan et al²⁷ demonstrated early uptake (24 hours) of superparamagnetic iron oxide nanoparticles (ferumoxytol) as a marker of macrophage infiltration in the vessel walls of cerebral aneurysms. These studies demonstrated associations with early intracranial aneurysm rupture, increased inflammatory mediators (cyclooxygenase-2, microsomal prostaglandin E2 synthase-1), and macrophages on histopathologic immunostaining.

Because atherosclerosis is an inflammatory process, transient identification of acute inflammation/plaque enhancement, rate of contrast permeability, intraplaque hemorrhage, and macrophage infiltration (potentially early ferumoxytol uptake) may serve as

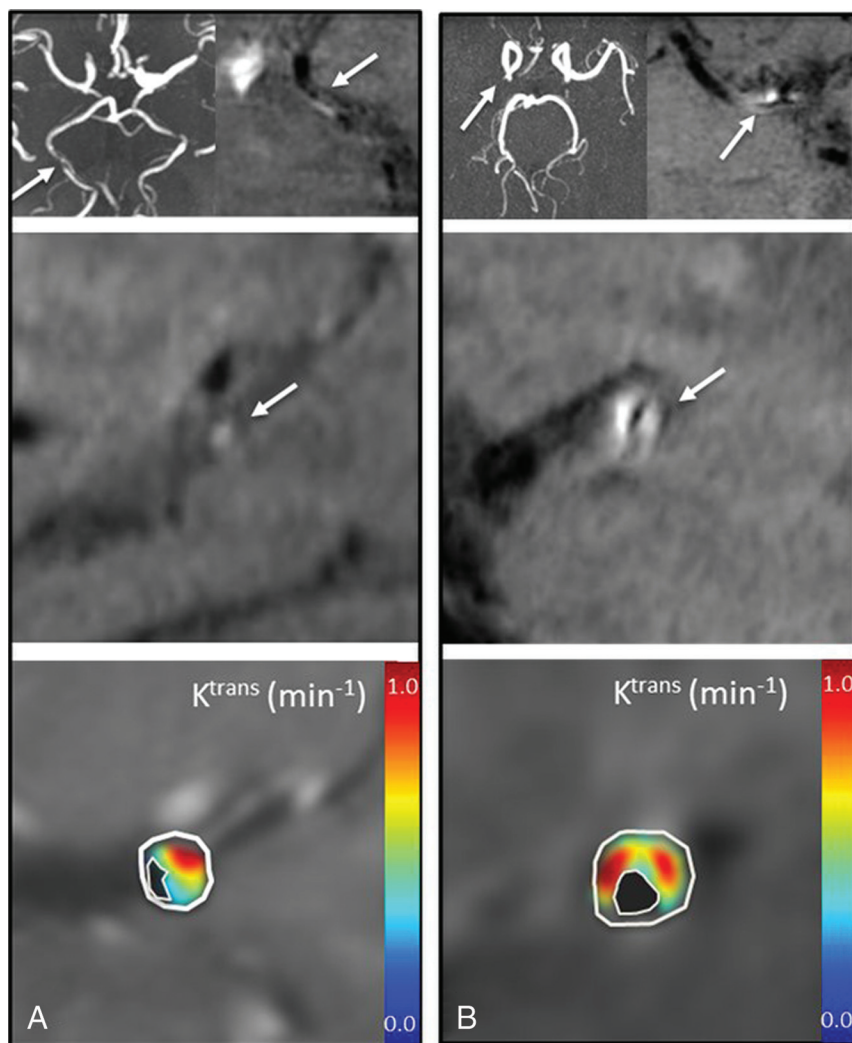


FIG 4. K^{trans} plaque permeability differs from relative signal enhancement in T1 SPACE imaging in 2 patients. Each panel shows axial TOF MRA (upper left), axial T1 SPACE (upper right), and sagittal T1 SPACE (middle) MR images confirming vessel patency with eccentric plaque, and K^{trans} (lower). A, A 69-year-old man with right posterior cerebral artery stenosis on TOF MRA and corresponding T1 SPACE plaque enhancement measured at 123%. K^{trans} measured at 0.39 minutes⁻¹, and V_p at 11%. B, A 54-year-old woman with right MCA stenosis and corresponding T1 SPACE plaque enhancement measured at 226%, K^{trans} measured at 0.45 minutes⁻¹, and V_p at 12%.

MR imaging markers to characterize and grade the acute vulnerability of these lesions to thromboembolic/perforator ischemic complications. Even chronic progressing intracranial stenoses may be exacerbated by episodes of plaque inflammation and, in a setting of poor collaterals, could also predispose to hypoperfusion-related ischemic complications irrespective of plaque instability. Differentiating these mechanisms of stroke in ICAD may modulate treatment of symptomatic ICAD in the future, whereby angioplasty/stent placement could be advocated, delayed, or contraindicated in favor of antiplatelets, anticoagulants, statins, or novel anti-inflammatory therapies.

Our study has several limitations. First, this pilot study included a relatively small sample size and no longitudinal follow-up, both of which should be addressed in subsequent studies. Additionally, the patient population was limited to subjects with symptomatic ICAD plaques with >50% stenosis. Examining

asymptomatic plaques and less stenotic lesions, stenoses, which may not be easily characterized by K^{trans} , will be an important subject for future research. Furthermore, the inability to image the plateau and washout phase of plaque contrast prevents accurate estimation of V_L . However, this scenario does not preclude accurate measurement of K^{trans} from the wash-in phase of the curve because V_L does not affect it. Finally, our model of K^{trans} contrast permeability into the intracranial plaque from the intravascular space to the extracellular extravascular space may be prone to variable mechanisms. Although neovascularization in pathologic ICAD may be a primary mode for plaque permeability/enhancement, passive diffusion from the intraluminal space across a compromised fibrous cap cannot be excluded, and these processes may vary across a spectrum of intracranial plaques.

CONCLUSIONS

We present the results of a prospective pilot study examining the feasibility of kinetic modeling of contrast uptake in ICAD. We demonstrate elevated and variable permeability in symptomatic atherosclerotic plaques (K^{trans} and V_p) less than levels observed in the choroid plexus where an absence of the blood-brain barrier allows intercompartmental tracer exchange. We also found that plaque permeability is more associated with the time from symptom onset than IPE or IPH ratios as measured on BBMRI via T1 SPACE vessel wall imaging. Coupled with the fact

that neither K^{trans} nor V_p strongly correlated with IPE or IPH, these findings suggest that permeability modeling of plaque contrast kinetics may provide a new imaging biomarker for ICAD plaque instability.

Disclosures: Charles G. Cantrell—RELATED: Grant: American Heart Association PRE20380810.* Timothy J. Carroll—RELATED: Grant: American Heart Association 14GRNT20380798*; National Institutes of Health IR21EB017928* and IR01NS089926*; Sameer A. Ansari—RELATED: Grant: American Heart Association 13GRNT17340018* and 14GRNT20380798*; National Institutes of Health IR21HL130969.* *Money paid to the institution.

REFERENCES

1. Chimowitz MI, Lynn MJ, Howlett-Smith H, et al; Warfarin-Aspirin Symptomatic Intracranial Disease Trial Investigators. Comparison of warfarin and aspirin for symptomatic intracranial arterial stenosis. *N Engl J Med* 2005;352:1305–16 CrossRef Medline
2. Chimowitz MI, Lynn MJ, Derdeyn CP, et al; SAMMPRIS Trial Inves-

- tigators. **Stenting versus aggressive medical therapy for intracranial arterial stenosis.** *N Engl J Med* 2011;365:993–1003 [CrossRef Medline](#)
3. Swartz RH, Bhuta SS, Farb RI, et al. **Intracranial arterial wall imaging using high-resolution 3-Tesla contrast-enhanced MRI.** *Neurology* 2009;72:627–34 [CrossRef Medline](#)
4. Skarpathiotakis M, Mandell DM, Swartz RH, et al. **Intracranial atherosclerotic plaque enhancement in patients with ischemic stroke.** *AJNR Am J Neuroradiol* 2013;34:299–304 [CrossRef Medline](#)
5. Qiao Y, Steinman DA, Qin Q, et al. **Intracranial arterial wall imaging using three-dimensional high isotropic resolution black blood MRI at 3.0 Tesla.** *J Magn Reson Imaging* 2011;34:22–30 [CrossRef Medline](#)
6. Xu WH, Li ML, Gao S, et al. **Plaque distribution of stenotic middle cerebral artery and its clinical relevance.** *Stroke* 2011;42:2957–59 [CrossRef Medline](#)
7. Qiao Y, Zeiler SR, Mirbagheri S, et al. **Intracranial plaque enhancement in patients with cerebrovascular events on high-spatial-resolution MR images.** *Radiology* 2014;271:534–42 [CrossRef Medline](#)
8. Kerwin W, Hooker A, Spilker M, et al. **Quantitative magnetic resonance imaging analysis of neovascularity volume in carotid atherosclerotic plaque.** *Circulation* 2003;107:851–56 [CrossRef Medline](#)
9. Espinosa-Heidmann DG, Reinosa MA, Pina Y, et al. **Quantitative enumeration of vascular smooth muscle cells and endothelial cells derived from bone marrow precursors in experimental choroidal neovascularization.** *Exp Eye Res* 2005;80:369–78 [CrossRef Medline](#)
10. Kerwin WS, Oikawa M, Yuan C, et al. **MR imaging of adventitial vasa vasorum in carotid atherosclerosis.** *Magn Reson Med* 2008;59:507–14 [CrossRef Medline](#)
11. Dong L, Kerwin WS, Chen H, et al. **Carotid artery atherosclerosis: effect of intensive lipid therapy on the vasa vasorum—evaluation by using dynamic contrast-enhanced MR imaging.** *Radiology* 2011;260:224–31 [CrossRef Medline](#)
12. Chen XY, Wong KS, Lam WW, et al. **Middle cerebral artery atherosclerosis: histological comparison between plaques associated with and not associated with infarct in a postmortem study.** *Cerebrovasc Dis* 2008;25:74–80 [Medline](#)
13. Fram EK, Herfkens RJ, Johnson GA, et al. **Rapid calculation of T1 using variable flip angle gradient refocused imaging.** *Magn Reson Imaging* 1987;5:201–08 [CrossRef Medline](#)
14. Deoni SC. **High-resolution T1 mapping of the brain at 3T with driven equilibrium single pulse observation of T1 with high-speed incorporation of RF field inhomogeneities (DESPOT1-HIFI).** *J Magn Reson Imaging* 2007;26:1106–11 [CrossRef Medline](#)
15. Fan Z, Zhang Z, Chung YC, et al. **Carotid arterial wall MRI at 3T using 3D variable-flip-angle turbo spin-echo (TSE) with flow-sensitive dephasing (FSD).** *J Magn Reson Imaging* 2010;31:645–54 [CrossRef Medline](#)
16. Tofts PS, Brix G, Buckley DL, et al. **Estimating kinetic parameters from dynamic contrast-enhanced T(1)-weighted MRI of a diffusible tracer: standardized quantities and symbols.** *J Magn Reson Imaging* 1999;10:223–32 [Medline](#)
17. Tofts PS, Kermode AG. **Measurement of the blood-brain barrier permeability and leakage space using dynamic MR imaging, 1: fundamental concepts.** *Magn Reson Med* 1991;17:357–67 [CrossRef Medline](#)
18. Provenzale JM, Wang GR, Brenner T, et al. **Comparison of permeability in high-grade and low-grade brain tumors using dynamic susceptibility contrast MR imaging.** *AJR Am J Roentgenol* 2002;178:711–16 [CrossRef Medline](#)
19. Jia Z, Geng D, Liu Y, et al. **Low-grade and anaplastic oligodendrogliomas: differences in tumour microvascular permeability evaluated with dynamic contrast-enhanced magnetic resonance imaging.** *J Clin Neurosci* 2013;20:1110–13 [CrossRef Medline](#)
20. Vakil P, Ansari SA, Cantrell CG, et al. **Quantifying intracranial aneurysm wall permeability for risk assessment using dynamic contrast-enhanced MRI: a pilot study.** *AJNR Am J Neuroradiol* 2015;36:953–59 [CrossRef Medline](#)
21. Cha S, Yang L, Johnson G, et al. **Comparison of microvascular permeability measurements, K(trans), determined with conventional steady-state T1-weighted and first-pass T2*-weighted MR imaging methods in gliomas and meningiomas.** *AJNR Am J Neuroradiol* 2006;27:409–17 [Medline](#)
22. Li KL, Zhu XP, Checkley DR, et al. **Simultaneous mapping of blood volume and endothelial permeability surface area product in gliomas using iterative analysis of first-pass dynamic contrast enhanced MRI data.** *Br J Radiol* 2003;76:39–50 [CrossRef Medline](#)
23. Kilgore DP, Breger RK, Daniels DL, et al. **Cranial tissues: normal MR appearance after intravenous injection of GD-DTPA.** *Radiology* 1986;160:757–61 [CrossRef Medline](#)
24. Moreno PR, Purushothaman KR, Sirol M, et al. **Neovascularization in human atherosclerosis.** *Circulation* 2006;113:2245–52 [CrossRef Medline](#)
25. Virmani R, Kolodgie FD, Burke AP, et al. **Atherosclerotic plaque progression and vulnerability to rupture: angiogenesis as a source of intraplaque hemorrhage.** *Arterioscler Thromb Vasc Biol* 2005;25:2054–61 [CrossRef Medline](#)
26. Kolodgie FD, Gold HK, Burke AP, et al. **Intraplaque hemorrhage and progression of coronary atheroma.** *N Engl J Med* 2003;349:2316–25 [CrossRef Medline](#)
27. Hasan D, Chalouhi N, Jabbour P, et al. **Early change in ferumoxytol-enhanced magnetic resonance imaging signal suggests unstable human cerebral aneurysm: a pilot study.** *Stroke* 2012;43:3258–65 [CrossRef Medline](#)